https://doi.org/10.5194/egusphere-2026-2733
Preprint. Discussion started: 29 May 2026

Rapid detection of centimeter-scale change in a Mars analog environment using ground-based mobile LiDAR

Sashank Vanga[1], Reid P. Perkins[1], Catherine D. Neish[1], Michael R. Zannetti[2], Brett B. Carr[3], Christopher W. Hamilton[3]

[1] Department of Earth Sciences, Western University, London, Ontario, Canada

[2] NASA Marshall Space Flight Center, Huntsville, Alabama, USA

[3] Lunar and Planetary Laboratory, The University of Arizona, Tucson, Arizona, USA

Correspondence to: Sashank Vanga (svanga2@uwo.ca)

Abstract. Landed missions to dynamic planetary surfaces require tools capable of measuring the small-scale topographic changes driven by active surface processes. A ground-based LiDAR scanner is one of the few instruments capable of detecting the centimeter-scale changes that are expected due to both natural processes such as wind erosion and sedimentary reworking, as well as artificial processes resulting from robotic/human exploration. At landing site scales, a ground-based LiDAR scanner on a mobile platform can collect cm-scale topographic information more efficiently than using a scanner on a stationary mount. To demonstrate the viability of mobile LiDAR for planetary missions, we conducted scans at a Mars analog site in central Iceland. Scans before and after a windstorm detected erosion and deposition of sand on the order of a few cm, with a detection threshold of ~1 cm. The ability of the mobile platform to collect data over extremely short timescales (<30 minutes) made it possible to conduct spontaneous scans to record opportunistic targets after the windstorm, while maintaining cm-scale resolution. This makes a compelling case for the inclusion of mobile LiDAR on future missions to explore planetary surfaces such as the Moon, Mars and Titan.

https://doi.org/10.5194/egusphere-2026-2733
Preprint. Discussion started: 29 May 2026

1. Introduction

Light Detection and Ranging (LiDAR) is a common means of acquiring high-resolution topographic data from diverse surface environments (Cremons, 2022; Dong and Chen, 2017). In planetary exploration, LiDAR has largely been limited to orbital-based applications (e.g., the Mars Orbiter Laser Altimeter, MOLA) for regional scale mapping and surveying purposes that typically produce maps with a spatial resolution of tens to hundreds of meters per pixel (Cremons, 2022). While meter-scale topography from stereo optical image pairs exists for few extraterrestrial bodies (e.g., Burns et al., 2012; Sutton et al., 2022), centimeter-scale topographic data for planetary surfaces is rare. On the lunar surface, cm-scale topographic data only exists for select regions at 3 of 6 Apollo sites (Helfenstein and Shepard, 1999), and the Chang'E 4 and 6 landing sites (Wu et al., 2021; Yan et al., 2025). These data were obtained using stereo photogrammetry which, unlike LiDAR, is dependent on external illumination. Although a growing list of confirmed and proposed planetary surface missions (e.g., Colaprete, 2021; Ulamec et al., 2023) aim to collect more cm to sub-cm resolution stereo imagery from across the Solar System, asteroid Bennu remains the only extra-terrestrial body to date with cm-scale LiDAR derived topographic data (Seabrook et al., 2022).

Numerous Earth-based applications have leveraged LiDAR technology to produce repeat topographic surveys with ultrafine (cm to sub-cm) precision using stationary mounts (Heritage and Hetherington, 2007; Jaboyedoff et al., 2012; Sutton et al., 2024). More recently, mobile LiDAR systems mounted on vehicles or backpacks have been introduced (e.g., Di Stefano et al., 2021; James and Quinton, 2014; Kukko, 2013). At landing site scales (10s to 100s of meters), mobile systems can capture cm to mm-scale detail up to 40 times faster than static topographic surveys, since it is not necessary to continually reposition the stationary instrument to limit shadowing (Di Stefano et al., 2021; James and Quinton, 2014). Rovers provide an obvious platform for the use of mobile LiDAR on planetary surfaces. Despite an increasing number of planetary landers and rovers aiming to utilize LiDARs, most are primarily equipped for guidance and navigation purposes (e.g., Huang and Xu, 2024; Setterfield et al., 2021), not geologic investigations. The absence of science-oriented LiDARs on planetary surfaces contributes to a lack of understanding of surface processes that dominate at sub-meter scales. The work presented here demonstrates the rapid survey capabilities of a ground-based mobile LiDAR system in detecting cm-scale change at a large sand sheet in Iceland, while highlighting potential use cases for other planetary surfaces.

2. Instrumentation and Methodology

The LiDAR system used in this study consists of a 1550 nm *Riegl VUX-1HA* sensor mounted on a backpack frame along with a Global Navigation Satellite System (GNSS) antenna and an Inertial Measurement Unit (IMU). The backpack configuration paired with a *Stonex S900* static GNSS receiver acting as a reference station allows for rapid topographic data acquisition from surfaces within a few hundred meters of a traversed path, while maintaining cm-level accuracy (Perkins et al., 2025). To test the utility of the mobile LiDAR system for acquiring cm-scale topographic data from a landing site scale region, we conducted a study at Holuhraun (Iceland). Holuhraun refers to a fissure-fed rift zone associated with the Bárðarbunga–Veiðivötn volcanic system located in central Iceland (Thordarson and Larsen, 2007), the latest eruption of which produced an 83.5 km^2 lava flow-field in 2014–2015 (Gudmundsson et al., 2016; Voigt et al., 2021). Due to its Arctic location, lack of vegetation, and presence of abundant volcanic products,

https://doi.org/10.5194/egusphere-2026-2733
Preprint. Discussion started: 29 May 2026

Holuhraun is considered a high-fidelity analog for Martian terrain (Carr et al., 2024; Gwizd et al., 2024; Voigt et al., 2025).

On July 24, 2022, an approximately 13,200 m^2 sand covered section along the northern margin of the Holuhraun lava flow-field (Fig. 1a; hereafter referred to as "sandramp") was scanned in <30 minutes using the backpack LiDAR. Following an intense windstorm on the morning of July 31, another <30-minute scan was performed at the same location on August 1, 2022. The windstorm subjected the area to gale force winds with sustained windspeeds over 16 m/s and gusts exceeding 20 m/s (Hadland et al., 2026), causing noticeable redistribution in sand cover (Figs. 1b, c). The raw data from the mobile LiDAR surveys were processed using the Inertial Explorer and Spatial Explorer software to obtain georeferenced 3-dimensional (3D) point clouds of the region before and after the windstorm. The point clouds were spatially downsampled to a minimum point spacing of 5 mm using CloudCompare (cloudcompare.org, v2.14) to reduce data volume. A smaller 175 m^2 region of interest (ROI) within the sandramp (Fig. 1a) was selected for further analysis using cloud-to-cloud differencing. The ROI was selected due to the presence of stationary objects (i.e., rocks and boulders), sand ripples and visually apparent topographic variations. Stationary objects within the scene act as points of reference between the scans and could potentially highlight patterns in sand depth variation. Both downsampled point clouds of the ROI contain over 5.2 million points with an average point density of ~31,000 points/m^2.

2.1. Registration and Uncertainty

For the 2022 LiDAR datasets, we registered the August 1st ('after') point cloud to the July 24th ('before') point cloud by manually picking nine corresponding point pairs on the tops of rocks and boulders, which were interpreted to be unchanged between the scans. The average distance between points on the undisturbed surfaces in the before and after point clouds represents the registration error between the clouds. We isolated these undisturbed surfaces using the Cloth Simulation Filtering (CSF) algorithm (Zhang et al., 2016) in CloudCompare. We then applied the Multiscale Model to Model Cloud Comparison method (M3C2, see following section; Lague et al., 2013) to calculate the distance between the isolated unchanged points in the before and after clouds. The mean vertical distance was 0.003 m (3 mm), and the mean horizontal distance was 0.0004 m (0.4 mm). This demonstrates that the registration error is dominated by vertical offsets with minimal impact from horizontal errors. We thus use only the vertical dimension when reporting results, allowing for direct representation of erosional and depositional changes.

2.2. Point Cloud Differencing

The detection of surface changes caused by the windstorm was conducted by differencing the before and after point clouds using the M3C2 algorithm (Lague et al., 2013). Recent studies utilized M3C2 to identify meter to cm-scale changes in ground-based LiDAR data from terrestrial analog sites including Holuhraun (Bretzfelder et al., 2025; Sutton et al., 2024). M3C2 operates on a reference point cloud by computing normal vectors of several surfaces at local scales and measuring the movement (or lack thereof) between points in the reference cloud and points in the compared cloud along each surface normal. The resulting cloud-to-cloud distances can have positive or negative values, enabling detection of elevation gain or loss. M3C2 also calculates a 95% confidence interval for the distance, based on the registration error of the point clouds and the local surface roughness (Lague et al., 2013).

https://doi.org/10.5194/egusphere-2026-2733
Preprint. Discussion started: 29 May 2026

We applied M3C2 to our point clouds in the vertical (z) direction using the before cloud as the reference. The normals were calculated within a spherical neighborhood of 16 cm in diameter centered on each point on the reference cloud and changes were identified within a cylinder of 8 cm in diameter projected around the surface normals, up to a maximum column depth of 1.1 m (see Lague et al., 2013 for an explanation of parameters). We used 0.003 m as the registration error and calculated the vertical distance between the clouds. Results were projected onto the July 24th cloud for visualization (Fig. 1d).

https://doi.org/10.5194/egusphere-2026-2733
Preprint. Discussion started: 29 May 2026

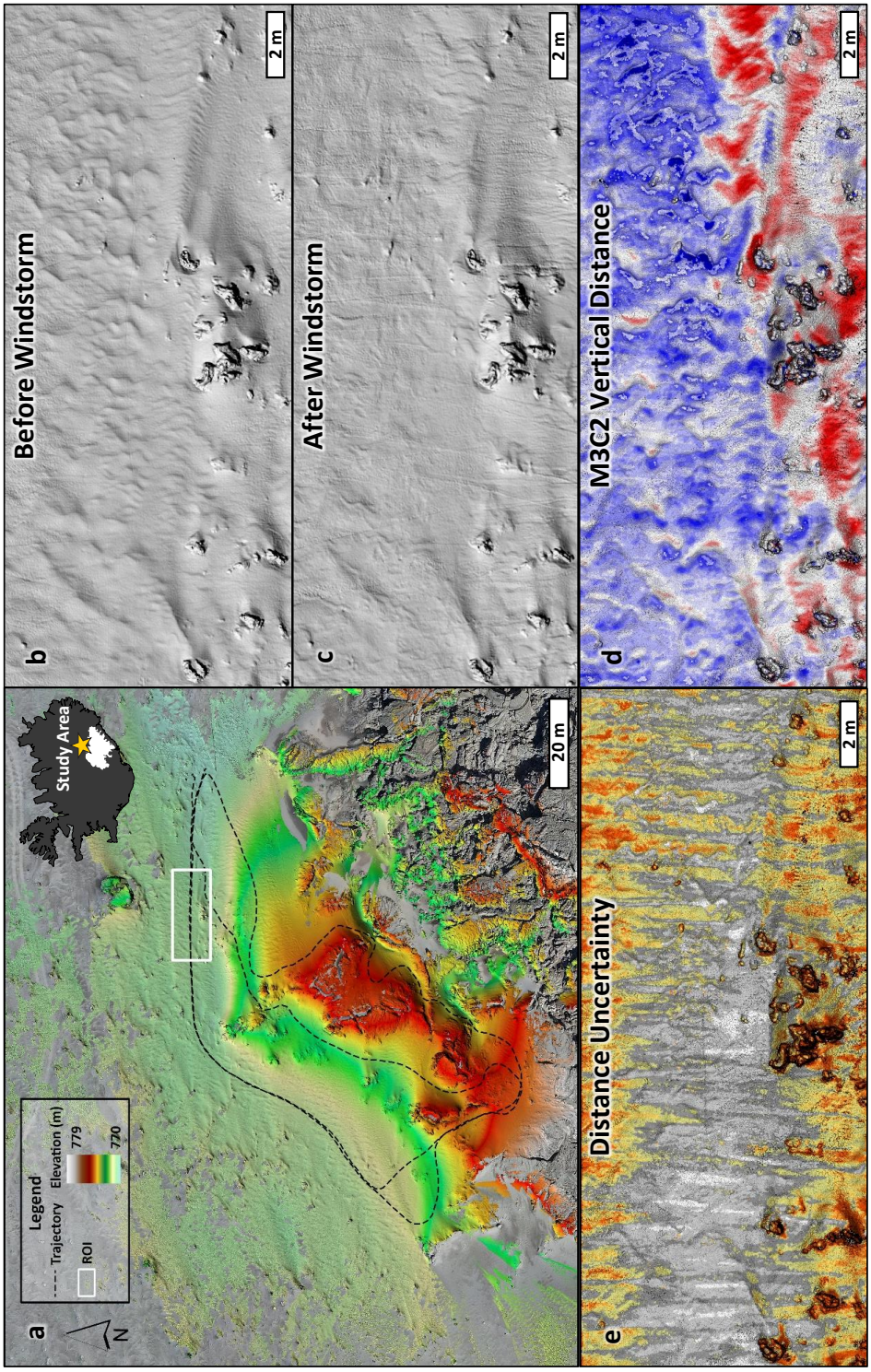

Figure 1: (a) July 24, 2022, LiDAR-derived colorized shaded relief map of the sandramp on the northern margin of the Holuhraun lava flow-field, showing the mobile LiDAR trajectory (dashed line) and ROI (white box, centered at 64.92005°N, 16.74503°W). The shaded relief map is overlaid on a UAS-derived orthoimage obtained on July 25, 2022 (Hamilton et al., 2026). The inset on the top-right shows a map of Iceland with Holuhraun's location indicated by a yellow star. (b) July 24, 2022, hillshade of the ROI at 1 cm/pixel resolution (before windstorm) and (c) August 1, 2022, hillshade of the ROI at 1 cm/pixel resolution (after windstorm). (d) M3C2 vertical distance map of the ROI, showing erosion (blue) and deposition (red) of sand between the July 24th and August 1st scans. White corresponds to regions with little to no change (±1 cm). The map represents change within ±8 cm, with darker colors indicating larger values. (e) M3C2 vertical distance uncertainty map of the ROI. The values range between 6.5 mm to >10 mm. Regions with uncertainty >9 mm are shown in orange, with darker colors indicating larger values. Regions with 8–9 mm of uncertainty are shown in yellow, and <8 mm are shown in grey, with lighter colors indicating smaller values.

https://doi.org/10.5194/egusphere-2026-2733
Preprint. Discussion started: 29 May 2026

3. Results

The before (Fig. 1b) and after (Fig. 1c) hillshades generated from 1 cm/pixel Digital Elevation Models (DEMs) provide an overview of the effects of the windstorm on the ROI. The cm-scale DEMs were rasterized from their respective point clouds by averaging height values within 0.01 m (1 cm) grids and interpolating to fill gaps. We utilized a similar rasterization process using the Volume Calculation tool in CloudCompare to measure the erosion and deposition volumes between the scans. We estimate the ROI experienced erosion of 2.03 m^3 and deposition of 1.07 m^3 between July 24 and August 1, 2022, resulting in a net erosion of 0.96 m^3 across the 175 m^2 region. Erosion within the ROI is evident from many sand ripples seen before the windstorm having been completely or partially removed after the windstorm (Figs. 1b, c).

The M3C2 vertical distance between the before and after clouds (Fig. 1d) shows the erosion of ripples in the north and center of the ROI (blue, Fig. 1d) and the deposition of sediment along the lava flow margin in the south of the ROI (red, Fig. 1d). Regions within ±1 cm of change are considered "no change" and are shown in white. Ripple migration in the prevalent wind direction (West to East), highlighted by alternating blue and red colors, is observed in the upper-left to upper-middle part of the scene. Maximum magnitudes of erosion and deposition across the ROI were on the order of 5–8 cm (Fig. 1d). While a larger portion of the ROI experienced decrease in sand depth after the windstorm, patterns of sand deposition appear to be more prevalent leeward of larger boulders (Fig. 1d).

Accounting for the vertical registration error of 3 mm, the uncertainty of the distance measurements at 95% confidence (Lague et al., 2013) for most points was <1 cm, with an average value of 8 mm, representing the approximate detection threshold of significant change in the ROI (Fig. 1e). Lower uncertainties (~6.5 mm) are found in the center of the ROI (light grey, Fig. 1e) and the largest uncertainties (>1 cm) are found on the edges of the ROI and around boulders (orange, Fig. 1e). Larger uncertainties likely stem from distance from the instrument location during the traverse (Fig. 1a) and the complex geometry of the rocks, causing extensive shadowing in LiDAR scans.

4. Discussion

Using point clouds derived from <30-minute mobile LiDAR scans, we identify cm-scale topographic changes caused by a windstorm in a Mars analog region located in Iceland. We measured change in surface elevation within a 1–8 cm threshold and movement of sand ripples, along a sand-covered volcanic margin within the study area. Through co-registration using GNSS-based and manual registration methods, we established an average uncertainty of 8 mm for the measured changes**.** We also calculated erosion and deposition volumes within the region of interest and identified a net decrease in sand volume between the scans. Our results demonstrate that it is possible to acquire cm-scale topographic data at landing site scales with a ground-based mobile LiDAR instrument in less than an hour; this is more efficient than data acquisition with comparable stationary instruments. High spatial resolution topographic data with well-constrained error will be instrumental to our understanding of the geologic processes occurring on other planets; these processes are imperceptible to orbital instruments, especially at sub-meter scales. Our work shows that the change detection methods demonstrated here can be applied to detect and quantify cm-scale change on other planetary surfaces, if the appropriate data is available. Equipping rovers with a mobile LiDAR scanner would allow them to efficiently acquire such data as they move about a planetary surface.

https://doi.org/10.5194/egusphere-2026-2733
Preprint. Discussion started: 29 May 2026

Combining cm-scale topographic data with existing multitemporal meter-scale remote sensing observations can help track the movement of aeolian features such as ripples and dunes (e.g., Bretzfelder et al., 2026). Our observations of what we perceive to be short-duration (~7 days) ripple migration identified in our scans could be particularly relevant to tracking similar features on Mars and Titan (Greeley et al., 2001; Marshall and Fenton, 2025). Topographic information collected at similar scales can also be useful in determining the effects of landing spacecraft on the Moon and Mars, which has implications for studying landing site alteration and related impacts due to planetary surface exploration (Jimenez Cuesta et al., 2025; Luo et al., 2023).

It is important to note that attaining cm-scale precision significantly depends on the ability to accurately register or "georeference" the collected data. For terrestrial LiDAR applications, this may be achieved through utilizing a combined GNSS/IMU configuration (Di Stefano et al., 2021; Pöppl et al., 2025) and use of ground control points (GCPs). Although no navigation framework similar to the Global Positioning System (GPS) currently exists for other planets, there are proposals aiming to change that in the near future (Esper et al., 2025; Zanotti et al., 2024). However, cm-scale topographic data can and has been collected in GPS-denied settings using specialized LiDAR mapping techniques (Di Stefano et al., 2021; Zanetti et al., 2022, 2023). Multitemporal data obtained through GPS-denied techniques may be co-registered with one another, with existing maps or orbital remote sensing data (e.g., Sutton et al., 2022) using georeferencing algorithms available in popular Geographic Information Systems (GIS) software packages (Hackeloeer et al., 2014; Kumar et al., 2023). Accurate information about localized scale and position can be obtained through co-registration of mobile LiDAR data collected in the absence of GNSS/GPS. This indicates that a similar system on another planet would be able to characterize surface changes similarly to that done with using a standard mobile LiDAR with GNSS.

5. Conclusion

The ability to accurately measure topographic features at multiple scales makes LiDAR a powerful tool for observing change on planetary surfaces. However, only a limited number of spacecraft currently utilize LiDARs for geologic investigations. Our work demonstrates the ability of a ground-based mobile LiDAR system to detect cm-scale wind-driven change at a landing site scale region in central Iceland, while highlighting the efficiency of mobile data acquisition over stationary tools. We use LiDAR-derived topographic data to identify cm-scale vertical change within the study area, while constraining the error to <1 cm. This indicates that minimizing error through careful co-registration would enable cm-scale change detection on planetary surfaces by LiDAR equipped landers and rovers, even in the absence of GPS. Our results have direct implications for studying fine-scale natural or exploration-driven phenomena encountered by landed assets on the surfaces of the Moon, Mars, and Titan. Overall, our work underscores the potential for ground-based mobile LiDAR systems to enhance scientific exploration of dynamic planetary surfaces by detecting change at centimeter scales in shorter timeframes than previously possible.

Data availability

LiDAR point clouds and DEMs from this study are made freely available through OpenTopography at doi.org/10.5069/G92805VK (Vanga et al., 2026)

https://doi.org/10.5194/egusphere-2026-2733
Preprint. Discussion started: 29 May 2026

Author contributions

SV: Writing – original draft, Writing – review & editing, Validation, Data curation, Formal analysis, Project administration, Investigation, Methodology

RPP: Writing – review & editing, Investigation, Methodology, Project administration

CDN: Conceptualization, Writing – review & editing, Supervision, Project administration, Methodology, Investigation, Funding acquisition

MRZ: Formal analysis, Methodology, Supervision, Writing – review & editing, Visualization, Conceptualization

BBC: Methodology, Writing – review & editing, Visualization, Formal analysis, Project administration

CWH: Investigation, Project administration, Validation, Visualization, Writing – review & editing, Methodology, Funding acquisition

Competing interests

The authors declare that they have no conflict of interest.

Acknowledgements

We thank the Vatnajökull National Park Service (Vatnajökulsþjóðgarður) for granting access to the Holuhraun area and sampling permits. We also thank the Icelandic Met Office (Veðurstofa Íslands) for providing weather data.

Financial support

This work was funded through a Canadian Space Agency (CSA) Flights and Fieldwork for the Advancement of Science and Technology (FAST) grant to CDN with partial support from the NASA Planetary Science and Technology through Analog Research (PSTAR) program (Grant #80NSSC21K0011). CWH and BBC acknowledge support from the University of Arizona Space Institute (UASI) for Simultaneous Localization And Mapping (SLAM) LiDAR for lunar exploration.

6. References

CloudCompare [software], https://cloudcompare.org/, 2025.

Bretzfelder, J.M., Zanetti, M., Day, M., Argueta, M.: The Martian Analog Bedforms of Death Valley National Park: Characterization and Multi-Scale Temporal Evolution. Presented at the 8th International Planetary Dunes Workshop, p. 3003. https://www.hou.usra.edu/meetings/dunes2025/pdf/3003.pdf, 2025.

Bretzfelder, J. M., Day, M., Argueta, M. O., Zanetti, M. R., Zimbelman, J. R., Getman, B., Widmer, J., Moon, S., Miller, K., and Whetsel, C.: The Ibex dune field of Death Valley National Park, California: Characterization and assessment for Use as a Martian analog, Aeolian Research, 75, 101032, https://doi.org/10.1016/j.aeolia.2026.101032, 2026.

Burns, K. N., Speyerer, E. J., Robinson, M. S., Tran, T., Rosiek, M. R., Archinal, B. A., Howington-Kraus, E., and the LROC Science Team: DIGITAL ELEVATION MODELS AND DERIVED PRODUCTS FROM LROC NAC STEREO OBSERVATIONS, The International Archives of the Photogrammetry, Remote Sensing and Spatial Information Sciences, XXXIX-B4, 483–488, https://doi.org/10.5194/isprsarchives-XXXIX-B4-483-2012, 2012.

Carr, B. B., Varnam, M., Hadland, N., Shah, J., Voigt, J. R. C., Gwizd, S., Stack, K. M., Calef, F., Francis, R., Basu, U., Björnsson, B., Chen, C. X., Dong, E., Moersch, J. E., Phillips, M., Springer, J., Neish, C. D., and Hamilton, C.

https://doi.org/10.5194/egusphere-2026-2733
Preprint. Discussion started: 29 May 2026

W.: Evaluating the Use of Unoccupied Aircraft Systems (UASs) for Planetary Exploration in Mars Analog Terrain, Planet. Sci. J., 5, 231, https://doi.org/10.3847/PSJ/ad781e, 2024.

Colaprete, A.: Volatiles Investigating Polar Exploration Rover (VIPER). https://ntrs.nasa.gov/citations/20210015009, 2021.

Cremons, D. R.: The future of lidar in planetary science, Front. Remote Sens., 3, https://doi.org/10.3389/frsen.2022.1042460, 2022.

Di Stefano, F., Chiappini, S., Gorreja, A., Balestra, M., and Pierdicca, R.: Mobile 3D scan LiDAR: a literature review, Geomatics, Natural Hazards and Risk, 12, 2387–2429, https://doi.org/10.1080/19475705.2021.1964617, 2021.

Dong, P. and Chen, Q.: LiDAR Remote Sensing and Applications, CRC Press, Boca Raton, 220 pp., https://doi.org/10.4324/9781351233354, 2017.

Esper, J., Heckler, G., Verville, J., Ryden, G.,: NASA's Lunar Communications Relay and Navigation Systems (LCRNS). Presented at the 18th International Conference on Space Operations, Montreal. https://ntrs.nasa.gov/citations/20250003321, 2025.

Greeley, R., Kuzmin, R. O., and Haberle, R. M.: Aeolian Processes and their Effects on Understanding the Chronology of Mars, Space Science Reviews, 96, 393–404, https://doi.org/10.1023/A:1011917910624, 2001.

Gudmundsson, M. T., Jónsdóttir, K., Hooper, A., Holohan, E. P., Halldórsson, S. A., Ófeigsson, B. G., Cesca, S., Vogfjörd, K. S., Sigmundsson, F., Högnadóttir, T., Einarsson, P., Sigmarsson, O., Jarosch, A. H., Jónasson, K., Magnússon, E., Hreinsdóttir, S., Bagnardi, M., Parks, M. M., Hjörleifsdóttir, V., Pálsson, F., Walter, T. R., Schöpfer, M. P. J., Heimann, S., Reynolds, H. I., Dumont, S., Bali, E., Gudfinnsson, G. H., Dahm, T., Roberts, M. J., Hensch, M., Belart, J. M. C., Spaans, K., Jakobsson, S., Gudmundsson, G. B., Fridriksdóttir, H. M., Drouin, V., Dürig, T., Aðalgeirsdóttir, G., Riishuus, M. S., Pedersen, G. B. M., van Boeckel, T., Oddsson, B., Pfeffer, M. A., Barsotti, S., Bergsson, B., Donovan, A., Burton, M. R., and Aiuppa, A.: Gradual caldera collapse at Bárdarbunga volcano, Iceland, regulated by lateral magma outflow, Science, 353, aaf8988, https://doi.org/10.1126/science.aaf8988, 2016.

Gwizd, S., Stack, K. M., Francis, R., Calef, F., Carr, B. B., Langley, C., Graff, J., Kristinsson, Þ. H., Thorarensen, V. P., Bernharðsson, E., Phillips, M., Varnam, M., Hadland, N., Shah, J., Moersch, J., Basu, U., Voigt, J. R. C., and Hamilton, C. W.: Comparing Rover and Helicopter Planetary Mission Architectures in a Mars Analog Setting in Iceland, Planet. Sci. J., 5, 172, https://doi.org/10.3847/PSJ/ad55f4, 2024.

Hackeloeer, A., Klasing, K., Krisp, J. M., and Meng, L.: Georeferencing: a review of methods and applications, Annals of GIS, 20, 61–69, https://doi.org/10.1080/19475683.2013.868826, 2014.

Hadland, N., Hamilton, C. W., Schroedl, P., Calabrese, F., Marlow, J., and Duhamel, S.: Microbial dispersal from a hyperactive sandsheet in the Icelandic Highland, Science of The Total Environment, 1025, 181659, https://doi.org/10.1016/j.scitotenv.2026.181659, 2026.

Hamilton, C. W., Carr, B. B., Voigt, J. R. C., and Scheidt, S. P.: Rover–Aerial Vehicle Exploration Network (RAVEN): Unoccupied Aircraft System (UAS) Surveys [data set], https://doi.org/10.25422/azu.data.27156978, 2026.

Helfenstein, P. and Shepard, M. K.: Submillimeter-Scale Topography of the Lunar Regolith, Icarus, 141, 107–131, https://doi.org/10.1006/icar.1999.6160, 1999.

Heritage, G. and Hetherington, D.: Towards a protocol for laser scanning in fluvial geomorphology, Earth Surface Processes and Landforms, 32, 66–74, https://doi.org/10.1002/esp.1375, 2007.

https://doi.org/10.5194/egusphere-2026-2733
Preprint. Discussion started: 29 May 2026

Huang, G. and Xu, W.: A Review of Lidar Technology in China's Lunar Exploration Program, Remote Sensing, 16, 4354, https://doi.org/10.3390/rs16234354, 2024.

Jaboyedoff, M., Oppikofer, T., Abellán, A., Derron, M.-H., Loye, A., Metzger, R., and Pedrazzini, A.: Use of LIDAR in landslide investigations: a review, Nat Hazards, 61, 5–28, https://doi.org/10.1007/s11069-010-9634-2, 2012.

James, M. R. and Quinton, J. N.: Ultra-rapid topographic surveying for complex environments: the hand-held mobile laser scanner (HMLS), Earth Surface Processes and Landforms, 39, 138–142, https://doi.org/10.1002/esp.3489, 2014.

Jimenez Cuesta, C., Davies, J., Worrall, K., Cammarano, A., and Zare-Behtash, H.: Plume-surface interactions: A review of experimental work, Acta Astronautica, 226, 892–912, https://doi.org/10.1016/j.actaastro.2024.09.021, 2025.

Kukko, A.: Mobile Laser Scanning – System development, performance and applications. Finnish Geodetic Institute. https://aaltodoc.aalto.fi/items/b85c6efc-9a06-4535-9067-78f80eddda3f, 2013.

Kumar, M., Singh, R. B., Singh, A., Pravesh, R., Majid, S. I., and Tiwari, A.: Referencing and Coordinate Systems in GIS, in: Geographic Information Systems in Urban Planning and Management, edited by: Kumar, M., Singh, R. B., Singh, A., Pravesh, R., Majid, S. I., and Tiwari, A., Springer Nature, Singapore, 25–46, https://doi.org/10.1007/978-981-19-7855-5_2, 2023.

Lague, D., Brodu, N., and Leroux, J.: Accurate 3D comparison of complex topography with terrestrial laser scanner: Application to the Rangitikei canyon (N-Z), ISPRS Journal of Photogrammetry and Remote Sensing, 82, 10–26, https://doi.org/10.1016/j.isprsjprs.2013.04.009, 2013.

Luo, P., Zhang, X., Liu, R., Zhang, M., Li, C., Xu, Y., Bugiolacchi, R., Hua, B., Zhang, H., Li, L., You, J., Xu, Y., Lei, L., Zou, X., Fu, Q., Wang, Y., Liang, X., Zhuang, J., Wang, L., Wang, Y., Wang, W., Feng, L., Liu, H., and Li, T.: Plume effects on Martian surface: Revealing evolution characteristics of plume-surface interaction at Tianwen-1 landing site, Engineering Geology, 325, 107278, https://doi.org/10.1016/j.enggeo.2023.107278, 2023.

Marshall, J. R. and Fenton, L. K.: Rolling stones on Titan, Planetary and Space Science, 258, 106076, https://doi.org/10.1016/j.pss.2025.106076, 2025.

Perkins, R. P., Hibbard, S. M., Neish, C. D., Hamilton, C. W., and Campbell, B. A.: Surface Properties of Sediments at the 2014–2015 Holuhraun Lava Flow-field: Insights from Multiwavelength Radar, Planet. Sci. J., 6, 259, https://doi.org/10.3847/PSJ/ae0b50, 2025.

Pöppl, F., Ullrich, A., Mandlburger, G., and Pfeifer, N.: Precise and efficient high-frequency trajectory estimation for LiDAR georeferencing, ISPRS Journal of Photogrammetry and Remote Sensing, 223, 344–361, https://doi.org/10.1016/j.isprsjprs.2025.03.007, 2025.

Seabrook, J. A., Daly, M. G., Barnouin, O. S., Palmer, E. E., Gaskell, R. W., Nair, H., and Lauretta, D. S.: Building a High-resolution Digital Terrain Model of Bennu from Laser Altimetry Data, Planet. Sci. J., 3, 265, https://doi.org/10.3847/PSJ/aca011, 2022.

Setterfield, T. P., Hewitt, R. A., Chen, P.-T., Espinoza, A. T., Trawny, N., and Katake, A.: LiDAR-Inertial Based Navigation and Mapping for Precision Landing, in: 2021 IEEE Aerospace Conference (50100), 2021 IEEE Aerospace Conference (50100), 1–19, https://doi.org/10.1109/AERO50100.2021.9438153, 2021.

Sutton, S. S., Chojnacki, M., McEwen, A. S., Kirk, R. L., Dundas, C. M., Schaefer, E. I., Conway, S. J., Diniega, S., Portyankina, G., Landis, M. E., Baugh, N. F., Heyd, R., Byrne, S., Tornabene, L. L., Ojha, L., and Hamilton, C. W.: Revealing Active Mars with HiRISE Digital Terrain Models, Remote Sensing, 14, 2403, https://doi.org/10.3390/rs14102403, 2022.

https://doi.org/10.5194/egusphere-2026-2733
Preprint. Discussion started: 29 May 2026

Sutton, S. S., Richardson, J. A., Whelley, P. L., Scheidt, S. P., and Hamilton, C. W.: Degradation of the 2014–2015 Holuhraun vent-proximal edifice in Iceland, Bull Volcanol, 86, 37, https://doi.org/10.1007/s00445-024-01709-9, 2024.

Thordarson, T. and Larsen, G.: Volcanism in Iceland in historical time: Volcano types, eruption styles and eruptive history, Journal of Geodynamics, 43, 118–152, https://doi.org/10.1016/j.jog.2006.09.005, 2007.

Ulamec, S., Michel, P., Grott, M., Böttger, U., Schröder, S., Hübers, H.-W., Cho, Y., Rull, F., Murdoch, N., Vernazza, P., Prieto-Ballesteros, O., Biele, J., Tardivel, S., Arrat, D., Hagelschuer, T., Knollenberg, J., Vivet, D., Sunday, C., Jorda, L., Groussin, O., Robin, C., and Miyamoto, H.: Science objectives of the MMX rover, Acta Astronautica, 210, 95–101, https://doi.org/10.1016/j.actaastro.2023.05.012, 2023.

Vanga, S., Perkins, R. P., Neish, C. D., Zanetti, M. R., Carr, B. B., and Hamilton, C. W.: Backpack LiDAR scans from a sand covered lava margin at Holuhraun (Iceland) [data set], https://doi.org/10.5069/G92805VK, 2026.

Voigt, J. R. C., Hamilton, C. W., Scheidt, S. P., Münzer, U., Höskuldsson, Á., Jónsdottir, I., and Thordarson, T.: Geomorphological characterization of the 2014–2015 Holuhraun lava flow-field in Iceland, Journal of Volcanology and Geothermal Research, 419, 107278, https://doi.org/10.1016/j.jvolgeores.2021.107278, 2021.

Voigt, J. R. C., Hamilton, C. W., Keszthelyi, L. P., Varnam, M., Hibbard, S. M., and Stack, K. M.: The 2014–2015 Holuhraun Lava Flow-field in Iceland as a Planetary Analog for Young Volcanic Terrains in Elysium Planitia, Mars, Planet. Sci. J., 6, 81, https://doi.org/10.3847/PSJ/adb5f1, 2025.

Wu, B., Li, Y., Liu, W. C., Wang, Y., Li, F., Zhao, Y., and Zhang, H.: Centimeter-resolution topographic modeling and fine-scale analysis of craters and rocks at the Chang'E-4 landing site, Earth and Planetary Science Letters, 553, 116666, https://doi.org/10.1016/j.epsl.2020.116666, 2021.

Yan, W., Zeng, X., Ren, X., Chen, W., Gao, X., Zuo, W., Liu, B., Zhang, Z., Fu, Q., Liu, J., and Li, C.: Geological characteristics of Chang'E-6 landing area in micro-scale unveiled by new observation data, Nat Commun, 16, 4219, https://doi.org/10.1038/s41467-025-59443-5, 2025.

Zanetti, M., Robinson, B., DeLeon Santiago, B., Hayward, E., Miller, K., Steiner, B., Draffen, A., Jetton, J., Walters, J., Kim, S., Bremner, P.: The Kinematic Navigation and Cartography Knapsack (KNaCK) LiDAR System: Overview and Applications. Presented at the 53rd Lunar and Planetary Science Conference, p. 2660. https://www.hou.usra.edu/meetings/lpsc2022/pdf/2660.pdf, 2022.

Zanetti, M.R., Neish, C.D., Miller, K., Bremner, P., Hayward, E., Adams, M., Perkins, R., Vanga, S., Hibbard, S.M., Hamilton, C.W.: Applications of Mobile LiDAR for Ultra-High Resolution and GPS-Denied Terrain Mapping in Planetary Analog Environments. Presented at the 54th Lunar and Planetary Science Conference, p. 2775. https://www.hou.usra.edu/meetings/lpsc2023/pdf/2775.pdf, 2023.

Zanotti, G., Ceresoli, M., Pasquale, A., Prinetto, J., and Lavagna, M.: High performance lunar constellation for navigation services to Moon orbiting users, Advances in Space Research, 73, 5665–5679, https://doi.org/10.1016/j.asr.2023.03.032, 2024.

Zhang, W., Qi, J., Wan, P., Wang, H., Xie, D., Wang, X., and Yan, G.: An Easy-to-Use Airborne LiDAR Data Filtering Method Based on Cloth Simulation, Remote Sensing, 8, 501, https://doi.org/10.3390/rs8060501, 2016.